Modeling and Simulation of a Three Phase Fixed Bed Catalytic Reactor for the Hydrogenation of 2-ethyl-hexenal

IONUT BANU*, EMIL FLORIN TUTA, GRIGORE BOZGA*
University Politehnica of Bucharest, Department of Chemical and Biochemical Engineering, 313 Splaiul Independentei, 060042 Bucharest, Romania

The aim of this work is the investigation, by modelling and simulation, of the liquid phase hydrogenation of 2-ethyl-2-hexenal to 2-ethyl-hexanol, over a modern Cu-Ni catalyst, in an industrial tri-phase trickle bed reactor. The chemical kinetics, hydrodynamic parameters and mass transfer coefficients were evaluated from published data. The mathematical model of the process takes into consideration intraparticle and interphase concentration gradients. The calculated temperature evolution along the catalytic reactor is in a good agreement with measured values from an industrial plant. The results indicate that critical kinetic step of the process is the hydrogen transfer toward the inner catalyst surface and that the process occurs close to gas-liquid equilibrium. The degree of catalyst pellet utilization, evaluated by internal effectiveness factors, is relatively low, being mainly dependent on rapid exhaust of dissolved hydrogen inside the catalyst pellet. The presented results could be useful in process analysis, optimization and control studies.

Keywords: Trickle-bed reactor, modeling and simulation, hydrogenation, nickel-copper catalyst, 2-ethyl-2-hexenal, 2-ethyl-hexanol

2-Ethyl-hexanol is one of the most important alcohols, used predominantly in the production of polymer plasticizers (dioctylphtalate and 1,2,4-trioctyltrimellitate), but also as a low volatility solvent, an intermediate in the synthesis of other organic products such as acrylic monomers used in the production of adhesives, dyes, paints and coating agents [1,2].

Industrially, 2-etilhexanol (2-HOL) is produced by liquid or gas phase hydrogenation of 2-ethyl-2-hexenal (2-HEL), a product of oxo-synthesis process. The reaction is catalyzed by copper chromium catalyst promoted with BaO, supported nickel (on kieselguhr or silica-alumina) or nickel Raney (sponge). The copper chromium catalyst has a better selectivity and presents a better thermal resistance, but is less active than nickel catalysts. Mixed Cu-Ni-Cr catalysts supported on silica or alumina were also prepared and tested in 2-HEL hydrogenation, being currently in commercial use [3,4]. Copper and nickel are largely used in hydrogenation processes of other organic compounds [5,6].

The 2-HEL hydrogenation process is involving two consecutive steps, the 2-HEL hydrogenation to 2-ethylhexanal (2-HAL) and the hydrogenation of the 2-HAL to 2-HOL. Some secondary reactions are also possible, but if the process is correctly operated, they have negligible intensities. The liquid phase hydrogenation process is less energy consuming, more selective and less exposed to catalyst deactivation as compared with that in gas phase.

The main chemical steps involved in the hydrogenation of 2-HEL are given in Fig. 1. Among the two intermediates, 2-ethylhexanal and 2-ethylhexenol, the rate of 2-ethylhexanal formation over the usual hydrogenation catalysts is much higher, the concentration of 2-ethylhexenol being negligible in technical calculations.

In spite of its importance, only few published studies are treating the kinetics of this process. Collins et al. [7] investigated the kinetics of 2-HEL hydrogenation to 2-HOL catalyzed by nickel Raney and nickel boride respectively, conducting the experiments in a slurry reactor. The authors reported a higher reactivity for carbon-carbon double bond, a total conversion of 2-HEL to 2-HOL in presence of nickel Raney and zero order kinetics for both hydrogenation steps. The kinetics of gas phase hydrogenation of 2-HEL to 2-HOL over a Ni/SiO_2 catalyst was investigated by Niklasson and Smedler [8]. The hydrogenation kinetic is described by a Langmuir-Hinshelwood model, where different active sites are involved in the occurrence of the two reaction steps.

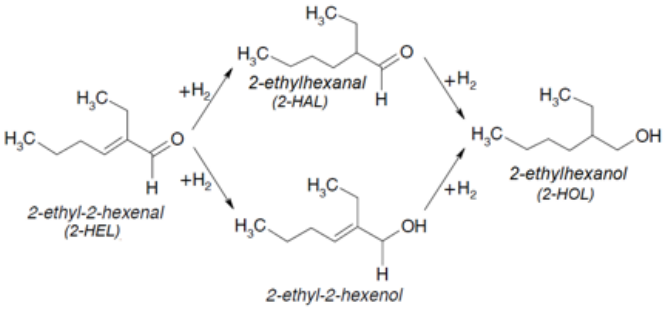

Fig. 1. The main reactions occurring in hydrogenation of 2-ethyl-2-hexenal to 2-ethylhexanol

Smedler [9] investigated the kinetics of 2-HEL hydrogenation on supported Ni, Ni-S and Pd catalysts, in liquid phase (slurry reactor). The author developed a Langmuir-Hinshelwood kinetic model for 2-HEL hydrogenation, hypothesizing the dissociative adsorption of hydrogen, mutual competition for active sites between hydrogen and the aldehydes, the controlling surface step being the chemical reaction of adsorbed species. Kinetic data for 2-HEL hydrogenation on the Ni/alumina catalyst were also published by Mattos et al. [10].

The analysis of the 2-HEL hydrogenation process at commercial scale, in unsteady state conditions, was investigated by Both et al. [11] based on the kinetics published by Smedler [9], valid for Ni/SiO_2 catalyst.

The aim of this study is to investigate theoretically, by modelling and simulation, the process of 2-HEL hydrogenation in a three phase trickle bed industrial reactor, over the modern $Ni-Cu/SiO_2$ catalyst. The process kinetics on this catalyst was investigated in one of our previous studies [6]. The simulation results are in good agreement

* Phone: (+40)726315459; e_mail: g_bozga@chim.upb.ro

with measured temperature data from an industrial reactor. At our best knowledge, there are not published studies of this nature, investigating the industrial 2-HEL hydrogenation process on this catalyst, based on a specific kinetic model.

Mathematical model of the hydrogenation process

The catalytic reactor considered in this study is a fixed bed gas-liquid-solid reactor, operated in steady state conditions. The gas feed consists of pure hydrogen and the liquid phase contains 2-HEL diluted with 2-HOL product, in order to limit the temperature increase along the reactor.

The gas and liquid flows co-currently in downward direction through the fixed bed of catalyst. The steady-state process mathematical model was built in the following hypotheses:

- plug flow of the two phases along the catalyst bed. The neglecting of axial mixing is justified by the high bed length to pellet size ratio (> 100);
- the reactor is operated adiabatically;
- the catalyst pellet is isothermal and the interphase temperature gradients are negligible small. These hypotheses are supported by the relatively high thermal conductivities of the liquid mixture and gaseous hydrogen respectively.

The model is constituted of mass and energy balance equations for the gas and liquid phases, pressure variation along the reactor and mass balance equations for porous catalyst pellet.

In the development of mass balance equations, the formation of 2-ethylhexenol is neglected, the only considered reactions being:

$$\text{2-HEL} + H_2 \rightarrow \text{2-HAL} \quad (r_1)$$
$$\text{2-HAL} + H_2 \rightarrow \text{2-HOL} \quad (r_2) \qquad (1)$$

The reaction rate expressions of the two reactions have the form [6]:

$$r_1 = k_1 C_A C_B; \qquad k_1 = 1.23310^{-3} \exp\left[4881.2\left(\frac{1}{T} - \frac{1}{403}\right)\right] \left[m^6 \cdot kmol^{-1} \cdot kg^{-1} \cdot s^{-1}\right]$$

$$r_2 = k_2 C_A, \quad (C_D > 0); \qquad k_2 = 1.35510^{-4} \exp\left[6472.7\left(\frac{1}{T} - \frac{1}{403}\right)\right] \left[m^3 \cdot kg^{-1} \cdot s^{-1}\right] \qquad (2)$$

The gas phase balance of hydrogen (A) is described by the equation:

$$\frac{dF_A^{(g)}}{dz} = -S_T a_V k_L (C_{AL}^* - C_{AL}); \quad z=0, \; F_A^{(g)} = F_{A,0} \qquad (3)$$

The liquid phase balances of hydrogen (A), 2-HEL (B) and 2-HAL (D) are given by the equations:

$$u_L \frac{dC_{AL}}{dz} = a_V k_L (C_{AL}^* - C_{AL}) - a_S k_{SA} (C_{AL} - C_{AS}); \quad z=0, \; C_{AL} = C_{AL,0} \qquad (4)$$

$$u_L \frac{dC_{BL}}{dz} = -a_S k_{SB} (C_{BL} - C_{BS}); \quad z=0, \; C_{BL} = C_{BL,0} \qquad (5)$$

$$u_L \frac{dC_{DL}}{dz} = a_S k_{SD} (C_{DS} - C_{DL}); \quad z=0, \; C_{DL} = C_{DL,0} \qquad (6)$$

The liquid phase concentration of 2-HOL (F) is calculated from the stoichiometric relation:

$$C_{BL} + C_{DL} + C_{FL} = C_{BL,0} + C_{DL,0} + C_{FL,0} \qquad (7)$$

The liquid phase concentration of hydrogen at equilibrium, C^*_{AL}, is calculable from equilibrium molar fraction, calculated as described below (22). These equations are obtained assuming the liquid density constant along the reactor, an acceptable hypothesis considering the overall accuracy for evaluation of the model parameters by available correlations.

The overall heat balance along the bed is given by the equation:

$$\frac{dT}{dz} = \frac{S_T \rho_{bed} [(-\Delta H_{R1}) \eta_i^{(1)} r_{1,s} + (-\Delta H_{R2}) \eta_i^{(2)} r_{2,s}]}{F_m^{(g)} c_p^{(g)} + F_m^{(L)} c_s^{(L)}} \qquad (8)$$

The pressure drop along the reactor was calculated by the equation proposed by Ellman et al. [12], applicable for high interaction hydrodynamic regime ($X_G < 0.8$) and operating pressure in the range 1-100 bar:

$$\left(\frac{dP}{dz}\right)_{GL} = -f_{LGG} \frac{2 \rho_G u_G^2}{d_h} \qquad (9)$$

$$f_{LGG} = 6.96 (X_G \xi)^{-2} + 53.27 (X_G \xi)^{-1.5}; \qquad d_h = d_{pe} \left[\frac{16 \varepsilon^3}{9 \pi (1-\varepsilon)^2}\right]^{0.33} \qquad (10)$$

$$X_G = \frac{u_G}{u_L} \sqrt{\frac{\rho_G}{\rho_L}}; \quad \xi = \frac{Re_L^{0.25} We_L^{0.2}}{(1 + 3.17 Re_L^{1.65} We_L^{1.2})^{0.1}}; \qquad (11)$$

As known, the fixed bed gas- liquid–solid reactors with the two fluids flowing downward can be operated in four hydrodynamic regimes: trickle flow, spray flow, pulsed flow and bubble flow. A method for identifying the hydrodynamic regime for non-foaming mixtures is proposed by Charpentier and Favier [13]. To apply this method, there are calculated the dimensionless groups:

$$\lambda = \sqrt{\frac{\rho_G \rho_L}{\rho_{air} \rho_{H2O}}}; \quad \psi = \frac{\sigma_{H2O}}{\sigma_L} \left(\frac{\mu_L}{\mu_{H2O}}\right)^{1/3} \left(\frac{\rho_{H2O}}{\rho_L}\right)^{1/3}; \quad \Phi = 4.76 + 0.5 \frac{\rho_G}{\rho_{air}} \qquad (12)$$

where:

$\rho_{air} = 1.2 kg\ m^{-3}$; $\rho_{H2O} = 1000 kg\ m^{-3}$; $\sigma_{H2O} = 0.074\ N\ m^{-1}$; $\mu_{H2O} = 0.001$ Pas

By applying the Charpentier and Favier's method, it was found that the reactor operating conditions considered in this work (see next section), correspond to the pulse flow regime, being fulfilled the inequality:

$$\frac{L}{G} \frac{\lambda \psi}{\Phi} \geq \left(\frac{G}{\lambda}\right)^{-1.3} \qquad (13)$$

The efficiency of catalyst wetting (the fraction of the external surface area of the pellet, covered with liquid) and the liquid holdup of the bed were evaluated as averages of the correlations presented in table 1. Note that some of these correlations are including the pressure loss in the two phases, reported to the unit of bed height, $(\Delta/h)_G$ and $(\Delta/h)_L$, calculated by the Ergun equation [13]. Similarly, the liquid film hydrogen transfer coefficient (k_L) and the mass transfer coefficients, k_{SJ}, are calculated as averages of the correlations presented in table 2.

Using the Fick diffusion model, the balance equations of the hydrogen (A), 2-HEL (B), 2-HAL (D) and 2-HOL (F) inside the catalyst pellet, considered as an equivalent sphere, have the form:

$$\frac{D_{ef,J}}{x^2} \frac{d}{dx}\left(x^2 \frac{dC_J}{dx}\right) - R_p^2 \rho_p \sum_{k=1}^{2} (\nu_{kJ} r_k) = 0, \quad J = A,B,D,F \qquad (14)$$

$$x=0, \quad \frac{dC_J}{dx} = 0; \qquad x=1, \quad k_{SJ}(C_{JL} - C_{JS}) = \frac{1}{R_p} D_{ef,J} \frac{dC_J}{dx}$$

In the system of differential equations (14), only two are independent, the other two being related to the first

ones by stoichiometric relations. Consequently, by combining the differential balance equations (14) written for D and F with those for A and B, one obtains:

$$C_D = C_{DS} - \frac{D_{ef,A}}{D_{ef,D}}(C_{AS} - C_A) + \frac{2D_{ef,B}}{D_{ef,D}}(C_{BS} - C_B) \quad (15)$$

$$C_F = C_{FS} + \frac{D_{ef,A}}{D_{ef,F}}(C_{AS} - C_A) - \frac{D_{ef,B}}{D_{ef,F}}(C_{BS} - C_B) \quad (16)$$

The effective diffusion coefficients inside the porous catalyst pellet, corresponding to the molecular mechanism, were calculated by the relation:

$$D_{ef,J} = \frac{\varepsilon}{\tau} D_{J,m} \quad (17)$$

Considering the relatively large concentration of 2-HOL, the molecular diffusion coefficients for the hydrogen, 2-HEL and 2-HAL in the liquid mixture ($D_{J,m}$) were approximated by the binary diffusion coefficients of corresponding species in 2-HOL. Due to the similarity of molecules structure, the molecular diffusion coefficient of 2-HAL was considered equal with that of 2-HEL. The diffusion coefficient of hydrogen was calculated by Wilke-Chang method, whereas for the 2-HEL it was calculated as an average of the values predicted by the methods Tyn-Calus, Hayduk- Minhas and Wilke-Chang respectively, as described by Reid et al. [30].

The influences of internal diffusion on the two reactions kinetics were evaluated by the internal effectiveness factors, defined as:

$$\eta_i^{(k)} = \frac{\bar{r}_k}{r_{k,s}}, \quad k=1,2 \quad (18)$$

The average reaction rate on the volume of the catalyst pellet has the expression:

$$\bar{r}_k = \frac{1}{V_p}\int_0^{V_p} r_k(V)\,dV = 3\int_0^1 x^2 r_k(x)\,dx \quad (19)$$

The equations (14)-(16) were used to calculate the internal effectiveness factors of the catalyst pellet and the liquid concentrations at the catalyst surface, C_{jS}, appearing in the equations (3) to (7). When the values of the internal effectiveness factors are known, the liquid concentrations on the external catalyst surface can be calculated more simply by using the balance equations of species around the catalyst pellet:

Table 1

CORRELATIONS USED FOR THE EVALUATION OF HYDRODYNAMIC PARAMETERS

Relation	Authors
$f = \tanh\left[3.03 Re_L^{0.375} Fr^{0.312} We_L^{-0.122}\left(\frac{a_S d_{pe}}{\varepsilon^2}\right)^{-0.11}\right]$ $Fr = \frac{a_S L^2}{\rho_L^2 g}$; $We_L = \frac{L^2}{\sigma_L \rho_L a_S}$	Mills and Dudukovic [14]
$f = 1.617 Re_L^{0.146} Ga^{-0.071}$; $Ga = \frac{\rho_L^2 d_{pe}^3 g}{\mu_L^2}$	El-Hisnawi et al. [15]
$f = 1 - \exp(-644 u_L^{0.964})$	Ring and Missen [16]
$f = 0.468 L^{0.227} G^{0.153}$	Burghardt et al. [17]
$f = 1.104 Re_{L,m}^{0.333}\left\{\frac{1+[(\Delta P/h)_{GL}/(\rho_L g)]}{Ga_m}\right\}^{1.9}$; $Ga_m = Ga\frac{\varepsilon^3}{(1-\varepsilon)^3}$; $Re_{L,m} = \frac{Re_L}{1-\varepsilon}$ $(\Delta P/h)_{GL} = -\left(\frac{dP}{dz}\right)_{GL}$ calculated by relation (9)	Al-Dahhan and Dudukovic [18]
$f = 4.45 u_L^{0.27}$	Wu et al. [19]
$\frac{\varepsilon_{LS}}{\varepsilon} = 0.037 Bn^k$; $Bn = \frac{\rho_L g}{\sigma_L a_S^2}$; k=-0.07 for Bn<1 or k=-0.65 for Bn>1	Mersmann (1972), (see Ramachandran and Chaudhari [20])
$\frac{\varepsilon_{Ld}}{\varepsilon} = 2.021 Re_L^{0.344} Ga^{-0.197}$	El-Hisnawi et al. [15]
$\frac{\varepsilon_L}{\varepsilon} = 1 - 0.97\chi^{0.15}$; $\chi = \phi^{0.5} Re_G^{0.4} Re_L^{-1}$; $\phi = S_{ext}/d_{pe}^2$	Fukushima and Kusaka [21]
$\frac{\varepsilon_{Ld}}{\varepsilon} = 3.86 Re_L^{0.545} Ga^{-0.42}\left(\frac{d_{pe} a_S}{\varepsilon}\right)^{0.65}$	Specchia and Baldi [22]
$\frac{\varepsilon_L}{\varepsilon} = \frac{0.66 X^{0.81}}{1+0.66 X^{0.81}}$; $X = [\delta_L/\delta_G]^{0.5}$; $\delta_L = (\Delta P/h)_L$; $\delta_G = (\Delta P/h)_G$;	Midoux et al. [23]

$\log\left(\frac{\varepsilon_L}{\varepsilon}\right)=0.168\log X'-0.043\,(\log X')^2-0.363\,;\ X'=(\xi_L/\xi_G)^{0.5};$ $\xi_L=\frac{L}{\varepsilon}\left[\frac{1}{\rho_L}(\Delta P/h)_L+\rho_W\right];\ \xi_G=\frac{G}{\varepsilon}\left[\frac{1}{\rho_G}(\Delta P/h)_G+\rho_W\right];\ 0.05<X'<100$	Charpantier and Favier [13]
$a_V=175\,d_{pe}^{-0.8}u_L^{0.5}u_G^{0.6}$	Hirose et al. [24]
$\frac{a_V\,d_{pe}}{1-\varepsilon_L/\varepsilon}=0.059\,\phi^{-0.3}\,Re_L^{2/3}Re_G^{0.2};\ \phi=S_{ext}/d_{pe}^2$	Fukushima and Kusaka [21]
$\frac{a_V}{a_S}=1550\left[X_G Re_L^{-0.5}We\left(\frac{a_S\,d_h}{1-\varepsilon}\right)^{-5}\right]^{0.7};\ d_h=d_{pe}\left[\frac{16\,\varepsilon^3}{9\pi(1-\varepsilon)^2}\right]^{0.333}$	Wild et al. (1992) (see Iliuta et al. [25])

Table 2
CORRELATION USED FOR THE EVALUATION OF MASS TRANSFER COFFICIENTS

Relation	Authors
$\frac{k_L a_V d_{pe}^2}{D_J}=0.11Re_L\,Re_G^{0.4}Sc^{0.5}(d_R/d_{pe})^{0.3}$	Fukushima and Kusaka [26]
$k_L\,a_V=0.03\sqrt{E_L};\ E_L=(-\Delta P/h)_{GL}\,u_L$	Reiss [27]
$k_L\,a_V=353\sqrt{E_L D_{H2}};$	Saterfield [28]
$Sh'=0.71Ko^{0.21}Sc^{0.333};\ Sh'=\frac{k_{SJ}\,d_{pe}}{D_J};\ d_{pe}=\sqrt{\frac{S_{ext}}{\pi}}$	Rao and Drinkenburg [29]
$Sh_m=2.269\,Re_{mL}^{0.494}Re_{mG}^{0.178}Ga^{-0.276}Sc^{0.33};\ Sh_m=\frac{k_{SJ}\,\delta}{D_J}$ $\delta=\left(\frac{\mu_L^2}{\rho_L^2 g}\right)^{1/3};\ Re_{m\alpha}=\frac{u_\alpha\,\rho_\alpha}{a_S\,\mu_\alpha},\ \alpha=G,L$	Burghardt et al. [17]

$$a_S\,k_{SJ}(C_{JS}-C_{JL})=\rho_{bed}\sum_{k=1}^{2}(\nu_{kJ}r_{k,s}\eta_i^{(k)}),\ J=A,B,D,F \qquad (20)$$

Results and discussions

The mathematical model presented in the previous section was used in the simulation of an industrial reactor for hydrogenation of 2-HEL to 2-HOL, having the characteristics and the nominal operating conditions presented in table 3. The catalytic reactor is constituted of two identical catalyst beds placed in series, with an intermediary redistribution zone of the two fluids. As the composition, temperature and pressure variations in the redistribution zone are negligible small, from the view point of calculations, the system was treated as a single bed reactor. The liquid feed is constituted of 2-HEL diluted with 2-HOL product, whereas the gas feed is pure hydrogen.

The efficiency of catalyst wetting (the fraction, *f*, of the external surface area of the pellet, covered with liquid) was evaluated by several methods presented in table 1. The value predicted by the relation of Burghardt et al. [17] is around 0.63. All the other relations are predicting the value *f*=1, so we considered in calculations a complete wetting of catalyst pellet external surface.

One of the key hydrodynamic parameters of the trickle bed reactor is the liquid holdup, calculated by the relations presented also in table 1. As known, it has two components, corresponding to static and dynamic (flowing) conditions. The static component of liquid holdup, evaluated using the correlation proposed by Mersmann (see Ramachandran and Chaudhari [20]) proved to be negligible, compared with the dynamic component ($\varepsilon_{Ld}/\varepsilon_{Ls}\cong 17$)

Table 3
CHARACTERISTICS OF THE INDUSTRIAL REACTOR FOR LIQUID PHASE HYDROGENATION OF 2-HEL

Parameter	Value
Catalyst	Ni-Cu/SiO_2 (~ 16% Ni, ~ 7% Cu)
Height of the catalyst bed	2 x 14 m
Diameter of the catalyst bed	1 m
Size of catalyst pellets	Extrudates, diameter 4 mm, length 8 mm
Specific surface area	73.5 m^2/g
Average pore diameter	16.8 nm
Density of the catalyst pellet	1160 kg/m^3
Density of the catalyst bed	650 kg/m^3
Feed temperature of the mixture	112°C
Inlet pressure	41 bar
2-HEL concentration in the liquid feed	0.103 (kg/kg)
Hydrogen excess in the gas feed	20 %
Superficial velocity of the liquid	0.03 m/s
Superficial velocity of the gaseous hydrogen	0.0275 m/s

The simulation of the hydrogenation process occurring in the catalyst bed, consists in the alternative integration of the equations (1) -(7) and (12) -(14), performed by specialized Matlab® package functions. Considering the particularities of gas-liquid contacting before the feed to the catalyst bed, the hydrogen concentration in the liquid phase at the inlet of the bed is considered equal to the equilibrium value. The physical properties of the components were calculated using data and relations given by Reid et al. [30] and Yaws [31].

For the hydrogen solubility in the reaction mixture we used the data published by Roginskaia et al. [32], that we correlated by the relation:

$$H=1520\exp\left[629.77\left(\frac{1}{T}-\frac{1}{373}\right)\right]\ \text{bar} \qquad (21)$$

The composition of gaseous phase along the reactor, at equilibrium, was calculated using the relations:

- for hydrogen:

$$y_{H2}=H\,x_{H2}/P \qquad (22)$$

-for the other components of the mixture:

$$y_j=p_{j,sat}\,x_j/P \qquad (23)$$

$$\sum_{j=1}^{n_c} x_j=1\ ; \qquad \sum_{j=1}^{n_c} y_j=1 \qquad (24)$$

The results shown that, due to their low volatility and to relatively important working pressure, the concentrations of the C_8 organic compounds in the gas phase are negligible, the major component, hydrogen, having the molar fraction over 0.989 (fig. 2). Consequently, the resistance to the gas-liquid transfer of hydrogen is practically concentrated in the liquid phase.

The numerical integration convergence of the mass balance equations in the pellet (14) is faster on the first zone of the reactor and decreases with the rise of temperature, featuring convergence difficulties on the zone with higher temperature.

The concentration profiles inside the catalyst pellet, at two positions in the first zone of the catalyst bed, are presented in figure 3. As resulting from these diagrams, the chemical transformation inside the catalyst pellet is limited by the level of hydrogen concentration, which is significant only in the vicinity of external pellet surface, over a zone representing approximately 15 % of the pellet radius.

The 2-HAL concentration presents a maximum in the vicinity of the outer surface of the pellet, as result of

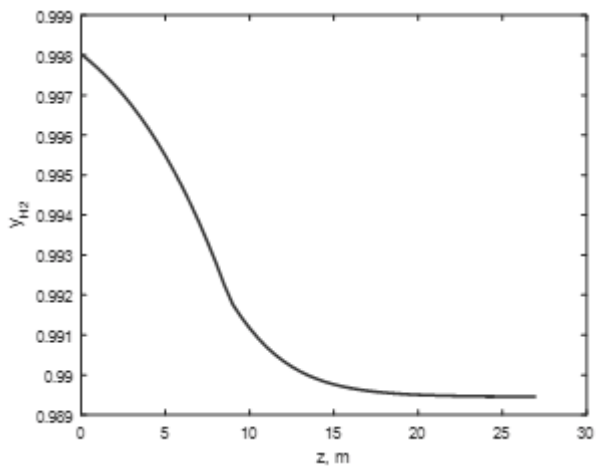

Fig. 2. Evolution of gas phase molar fraction of hydrogen along the hydrogenation reactor

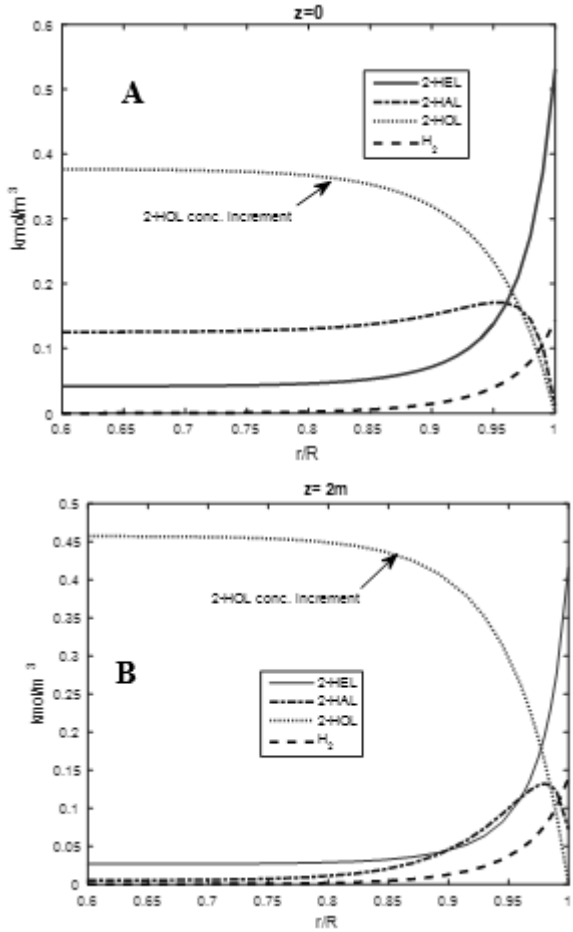

Fig. 3. Typical concentration profiles inside the catalyst pellet (there are represented only the pellet zones where the variations are significant). Note that for 2-HOL the curves represent the concentration increment in respect with the external surface (C_j-C_{jS}). **A**: z=0, $\eta_i^{(1)}$= 0.051, $\eta_i^{(2)}$= 0.112; **B**: z=2 m, $\eta_i^{(1)}$= 0.046, $\eta_i^{(2)}$= 0.107

cumulated influences of reactions and diffusion phenomena. However, the amplitude of this maximum is rather low due to the higher hydrogenation rate of the 2-HAL, as compared with 2-HEL hydrogenation one.

Typical values for the effectiveness factors of the two reactions, along the catalyst bed, in the described conditions, are $\eta_i^{(1)}$= 0.045 and $\eta_i^{(2)}$= 0.105, these indicating a weak efficiency of the catalyst utilization. The simulations were performed with these values of effectiveness factors, constant along the reactor.

The evolutions of 2-HEL, 2-HAL and 2-HOL concentrations along the catalyst bed are depicted in figure 4. As observed, the reactant (2-HEL) is practically consumed on the first half of the bed. The concentration profile of the intermediary hydrogenation product (2-HAL) presents a weak maximum, which is practically disappearing after the first third of the bed, due to the strong increase of its consumption rate with temperature.

As resulting from figure 4, the hydrogenation reaction is practically accomplished on the first 15 m of catalyst bed, the simulation data being specific for the operation of a fresh catalyst. In time, due to catalyst deactivation, the reaction zone is progressively extending to all the catalyst bed. Due to the lack of reliable catalyst deactivation data, in this study was not taken into consideration the deactivation phenomenon. The calculated evolution of temperature along the catalyst bed is represented in figure 5A, comparatively with measured values from an industrial reactor (Oltchim plant, Romania). The comparison of calculated and measured values of temperature evolutions

is evidencing a satisfactory quality of the trickle bed model described above. On the first half of the catalyst bed, the temperature is underestimated by maximum 4 K, whereas on the second zone, it is overestimated by maximum 3 K. Considering the direct dependency existing between temperature and composition along the adiabatic reactors, the adequacy of temperature predictions is proving also the appropriateness of composition predictions of the reactor model.

The calculated pressure drop along the catalyst beds is around 0.9 bar (Ffg. 5B). The evolution of liquid phase hydrogen concentration along the reactor is depicted in figure 6, as compared with values at thermodynamic equilibrium. These results are evidencing that the values of dissolved hydrogen concentrations, calculated considering the interphase mass transfer kinetics, are rather close to the ones corresponding to gas-liquid equilibrium, the maximum difference, of 6-7 %, occurring on the first

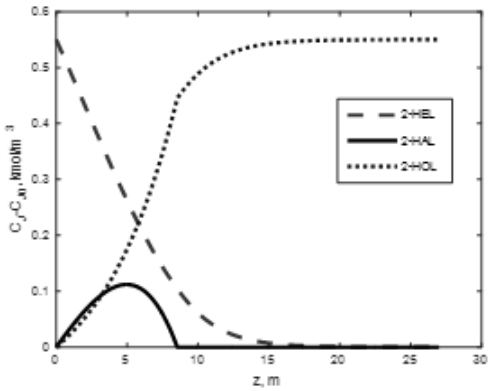

Fig. 4. Calculated liquid phase concentration profiles along the bed

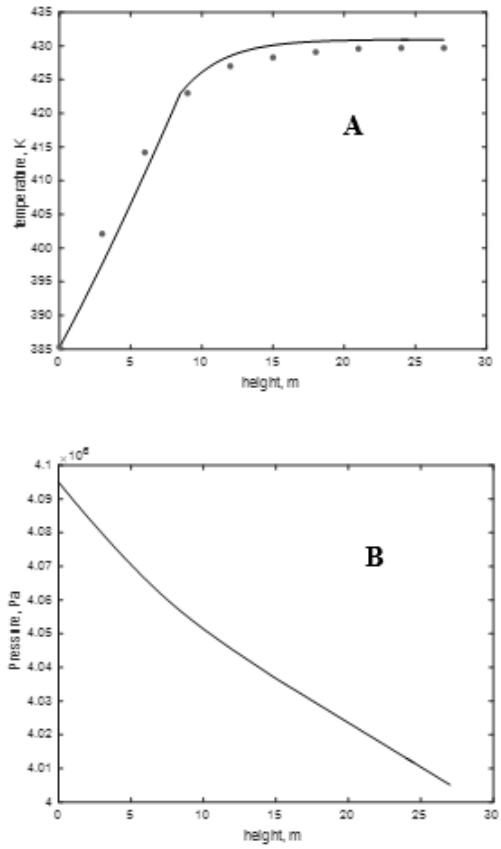

Fig. 5.Temperature (A) and pressure (B) evolutions along the reactor (solid line - calculated values; the points - measured temperature values)

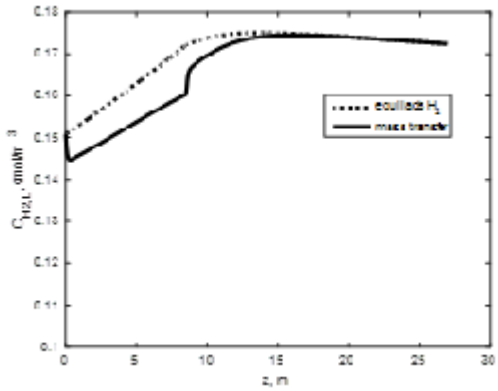

Fig. 6. Liquid phase hydrogen concentration calculated considering gas-liquid transfer kinetics (solid line) and as-liquid equilibrium (dashed line)

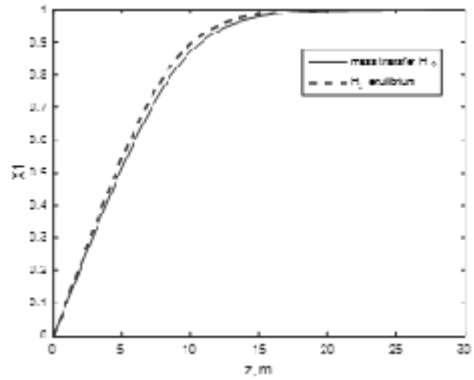

Fig. 7. 2-HEL conversion along the reactor calculated considering gas-liquid transfer kinetics (solid line) and gas-liquid equilibrium (dashed line)

third of the bed, where the overall hydrogenation consumption rate is maximal.

The evolutions of the 2-HEL conversion along the reactor, in the two cases, are given in figure 7. The closeness of the two curves indicates that, in the reactor simulation calculations, it can be used, without significant error, the hypothesis of gas-liquid equilibrium (eliminating the hydrogen balance equation in liquid phase (4)).

The sensitivity in respect with the model parameters

The mathematical model of the three phase hydrogenation reactor is characterized by an important number of parameters, evaluated from published correlations. The effect of the uncertainties in the calculation of these parameters on the model prediction accuracy was assessed by reactor simulations with perturbed values of parameters around the nominal values. The most significant results are presented graphically in the figures 8 to 10.

The most important sensitivity of the model prediction proved to be that in respect with the solubility parameter of hydrogen, H (fig. 8). This is explained by the process running close to hydrogen absorption equilibrium and the limiting influence of the dissolved hydrogen concentration on the process inside the catalyst pellet, evidenced above. Besides the solubility parameter, H, the hydrogen solubility in liquid phase is also dependent on the hydrogen pressure, evidenced by an important sensitivity in respect with this operating parameter (fig. 9). The sensitivity in respect with the effective diffusion coefficients (D_{ef}) is presented in figure 10. Even smaller than the sensitivity in respect with the hydrogen solubility parameter, H, the sensitivity in respect with D_{ef} is significant. The region of maximum sensitivity is comprised between 5 and 15 m, where the

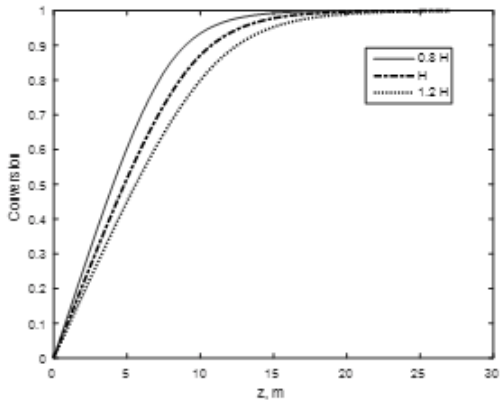

Fig. 8. Sensitivity of the 2-HEL conversion in respect with the hydrogen solubility parameter (H- the value for nominal operating conditions)

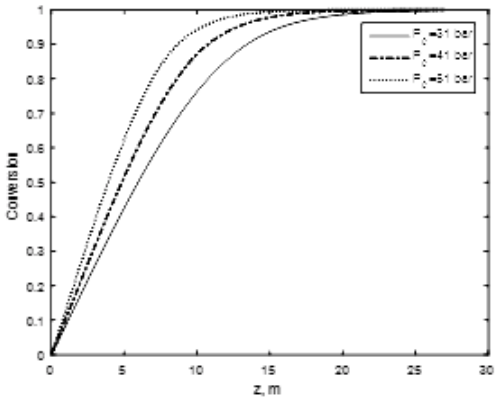

Fig. 9. Sensitivity of the 2-HEL conversion in respect with inlet pressure of the hydrogen

temperature increase is maximal (fig. 9). Note that, in this figure, D_{ef} is the vector of components $D_{ef,A}$ and $D_{ef,B}$.

The sensitivity in respect with the gas-liquid mass transfer coefficient of hydrogen and liquid-solid mass transfer coefficients of hydrogen and 2-HEl are much lower (fig. 11). This result is evidencing that the uncertainties in the evaluations of the mass transfer coefficients, k_L and k_S, do not influence significantly the model predictions in the simulated conditions. These are indicating that the limiting factor of the hydrogenation process is the hydrogen solubility in the liquid reaction mixture and lesser its transport inside the catalyst pellet. A means to increase the hydrogen solubility is to increase the working pressure. However, this is directly influencing the energy consumption of the plant.

Conclusions

The paper presents a modelling and simulation study for the process of 2-ethyl-hexenal hydrogenation to 2-ethyl-hexanol, in a three phase trickle bed industrial reactor, over the modern Ni-Cu/SiO_2 catalyst. The simulation results are in a good agreement with measured temperature values from an industrial plant. They are indicating that the reactor is working at conditions close to gas-liquid equilibrium and the process bottleneck is the hydrogen provision to the active sites of catalyst surface. This is depending mainly on the hydrogen solubility in liquid phase, directly related to the working pressure. The results evidenced also a weak dependence of the model predictions on the interphase mass transfer coefficients. The degree of catalyst pellet utilization appears rather low and is limited by the rapid exhaust of hydrogen inside the catalyst pellet.

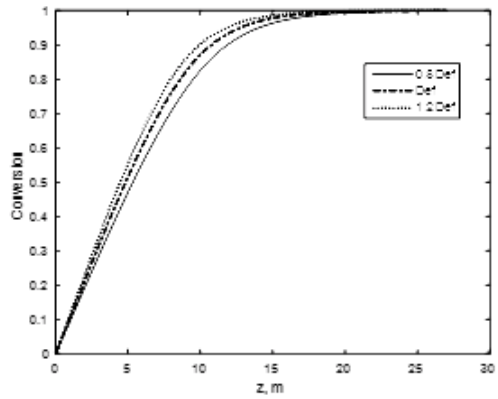

Fig. 10. Sensitivity of the 2-HEL conversion in respect with the reactant effective diffusion coefficients inside the catalyst pellet (D_{ef}- the values for nominal operating conditions)

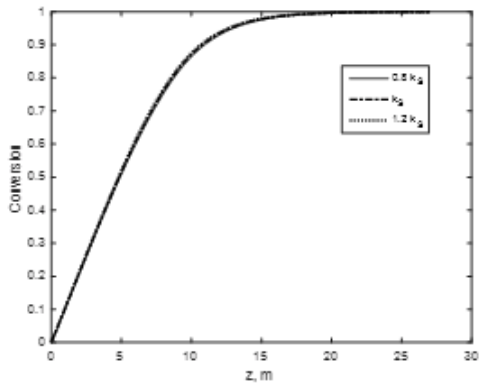

Fig. 11. Sensitivity of the 2-HEL conversion in respect with the liquid-solid mass transfer of reactants (k_S -the value for nominal operating conditions)

Notations

a_S-liquid-solid interfacial area reported to unit volume of packed bed, m^{-1};

a_V-gas-liquid interfacial area reported to unit volume of packed bed, m^{-1};

C^*_{AL}- dissolved concentration of hydrogen on the gas-liquid interface (assumed at equilibrium state with the gas phase), kmol m^{-3};

C_j- - concentration of j inside the catalyst pellet, kmol m^{-3};

C_{jL}- - bulk liquid phase concentration of species j, kmol m^{-3};

C_{jS}- - liquid phase concentration of j on external surface of catalyst pellet, kmol m^{-3};

$c_p^{(g)}$, $c_s^{(L)}$- specific heats of gas and liquid mixture respectively, J kg^{-1} K^{-1};

$D_{ef,j}$-effective diffusion coefficient for species j inside the porous pellet, m^2 s^{-1};

$D_{J,m}$-molecular diffusion coefficient in liquid phase, m^2s^{-1};

$d_{pe} = \sqrt{S_{ext}/\pi}$ - equivalent diameter of catalyst pellet, m;

f - wetting efficiency of the catalyst pellet (fraction of the external surface area of the pellet, covered with liquid);

$F_A^{(g)}$ -hydrogen flowrate in the gas phase, kmol s^{-1};

Δ_{HR1}, Δ_{HR1} -mass flowrates of gas and liquid respectively, kg s^{-1};

g-acceleration due to gravity, m s^{-2};

G, L- specific mass flowrate of gas and liquid respectively, kg m^{-2} s^{-1};

H-Henry constant for hydrogen solubility, bar;

ΔH_{R1}, ΔH_{R2} - enthalpy variations in the two considered reactions, J $kmol^{-1}$;

k_L-mass transfer coefficient for hydrogen through the liquid film adjacent to gas-liquid interface, m s^{-1};

k_{Sj}- liquid-solid mass transfer coefficient of species j, m s^{-1};

P- pressure, Pa;

$P_{j,sat}$ - vapor pressure of species j at equilibrium (saturation), Pa;
$(\Delta P/h)_G$, $(\Delta P/h)_L$ - pressure loss in the two fluids, reported to the unit of height, Pa m^{-1};
$R_p = d_{pe}/2$ - radius of the catalyst pellet, m;
r_i- rate of reaction i, kmol kg_{cat}^{-1} s^{-1};
$r_{i,s}$- rate of reaction i, calculated at the external pellet surface, kmol kg_{cat}^{-1} s^{-1};
S_{ext}-external surface area of the catalyst pellet, m^2;
S_T- cross sectione area of the catalyst bed, m^2;
T- temperature, K;
u_α-superficial flow velocity of the phase α, m s^{-1};
V_p- volume of the catalyst pellet, m^3;
$x = r/R_p$- dimensionless radial coordinate inside the catalyst pellet;
z- axial coordinate of the catalyst bed, s;

Greek letters
ε- packed bed void fraction;
ε_L, ε_{LS} and ε_{Ld}-total, static and dynamic liquid holdup per unit volume of packed bed ;
$\eta_i^{(k)}$- internal effectiveness factor for the reaction k;
μ_α- dynamic viscosity of the phase α, kg m^{-1} s^{-1};
ν_{kj}- stoichiometric coefficient of species j in reaction k (negative for reactants);
ρ_α- density of the phase α, kg m^{-3};
ρ_{bed}- bulk density of the catalyst bed, kg m^{-3};
σ_L- surface tension of the liquid, Nm^{-1};
$\tau = 2$- tortuosity factor of the catalyst pellet.

Dimensionless numbers

$Ga = \rho_L^2 d_{pe}^3 g/\mu_L^2$ - Galileo number;

$Re_\alpha = \rho_\alpha u_\alpha d_{pe}/\mu_\alpha$ - Reynolds number for the phase α;

$Sc = \dfrac{\mu_L}{\rho_L D_j}$ - Schmidt number;

$We = u_L^2 d_{pe} \rho_L / \sigma_L$ - Weber number;

Abbreviations

2-HAL	- 2-ethyl-2-hexanal;
2-HEL	- 2-ethyl-2-hexenal;
2-HOL	- 2-etilhexanol;

Subscripts
0 – feed conditions; A – H_2; B - 2-HEL; D - 2-HAL; F- 2-HOL;
G –gas phase; L- liquid phase.

References

1. YUAN, L., HUI-FENG, X., Finance Research, **1**, 2012, March (http://researchpub.org/journal/fr/number/vol1-no2/vol1-no2-1.pdf)
2. TUTA, E. F.; BOZGA, G., Ind. Eng. Chem. Res., **50**, 2011, p. 4545.
3. LUEKEN, H. G., TANGER, U., DROSTE, W., LUDWI, G., GUBISCH D., U.S. Patent 4968 849, 1990.
4. TUTA, E. F., BOZGA, G., Rev. Chim. (Bucharest), **65,** no. 5, 2014, p. 603.
5. ARGESANU, C., BOMBOS, D. ,MATEI, V., JUGANARU, T., BOMBOS, M., VASILIEVICI, G., Rev. Chim. (Bucharest), **65**, no. 11, 2016, p. 1391
6. BOMBOS, D. , VELEA, S., BOMBOS, M., VASILIEVICI, G., ROSCA, P., Rev. Chim. (Bucharest), **67**, no. 10, 2014, p. 2034
7. COLLINS, D. J., GRIMES, D. E., DAVIS, B.H., Can. J. Chem. Eng., **61**, 1983, p. 36.
8. NIKLASSON, C., SMEDLER, G., Ind. Eng. Chem. Res., **26,** 1987, p. 403.
9. SMEDLER, G., Can. J. Chem. Eng., 67, 1989, p. 51.
10. MATTOS, A.R.J.M., PROBST, S.H., AFONSO, J.C., SCHMAL. M., J. Braz. Chem. Soc., 15, 2004, p. 760.
11. BOTH, R., CORMOS, A.-M., AGACHI, P.-S., FESTILA C., Comput. Chem. Eng., **52,** 2013, p. 100.
12. ELLMAN, M.J., MIDOUX, N., LAURENT, A., CHARPENTIER, J.C., Chem. Eng. Sci., **43,** 1988, p. 2201.
13. CHARPANTIER, J. C., FAVIER M., AIChE J., **21,** 1975, p. 1213.
14. MILLS, P. L., DUDUKOVIC M. P., AIChE J., 27, 1981, p. 893.
15. EL-HISNAWI, A.A., DUDUKOVIC, M.P., MILLS, P.L., ACS Symp. Ser., **196,** 1982, p. 421.
16. RING, Z.E., MISSEN, R.W., Can. J. Chem. Eng., **69,** 1991, p. 1016.
17. BURGHARDT, A., BARTELMUS, G., JAROSZYBKI, M., KOFODZIEJ, A., The Chem. Eng. J., **58**, 1995, p. 83.
18. AL-DAHHAN, M. H., DUDUKOVIC, M. P., Chem. Eng. Sci., **50,** 1995, p. 2377.
19. WU, Q., HU, X., YUE, P. L., WANG D., 17th Int. Symp. of Chem. Reaction Eng., Hong Kong, 2002 (accessible on line: http://repository.ust.hk/ir/bitstream/1783.1-3206/1/measur.PDF).
20. RAMACHANDRAN, P. A., CHAUDHARI, R. V., Three Phase Catalytic Reactors, 1983, Gordon and Breach, New York.
21. FUKUSHIMA, S., KUSAKA, K., J. Chem. Eng. Jpn., **10,** 1977a, p. 461.
22. SPECCHIA, V., BALDI, G., Chem. Eng. Sci., **32,** 1977, p. 515.
23. MIDOUX, N., FAVIER, M., CHARPENTIER, J.-C., J. Chem. Eng. Jpn., **9,** 1976, p. 350.
24. HIROSE, T., TODA, M., SATO, Y., J. Chem. Eng. Jpn., **7,** 1974, p. 187.
25. ILIUTA, I., LARACHI, F., GRANDJEAN, B.P.A., WILD G., Chem. Eng. Sci., **54,** 1999, p. 5633.
26. FUKUSHIMA, S.; KUSAKA, K., J. Chem. Eng. Jpn., **10**, 1977b, p. 468.
27. REISS, L. P., Ind. Eng. Chem. Proc. DD, **6,** 1967, p. 486.
28. SATTERFIELD, C. N., AIChE J., **21,** 1975, p. 209.
29. RAO, V. G., DRINKENBURG, A. A. H., AIChE J., **31**, 1985, p. 1059.
30. REID, R. C., PRAUSNITZ, J. M., POLING B. E., The Properties of Gases and Liquids, 4th edition, 1987, McGraw-Hill, New York.
31. YAWS, C. L., Thermophysical properties of chemicals and hydrocarbons, 2008, Wiliam Andrew Inc., Norwich.
32. ROGINSKAIA, N. G., TIURIKOVA, N.G., NECITAILO, N.L., Him. Prom., 1, 1979, p. 21.

Manuscript received:

Manuscript received: 9.05.2017